Synthesis and Structure−Property Relationships of Random and Block Copolymers: A Direct Comparison for Copoly(2-oxazoline)s

Martin W. M. Fijten,[†] Johannes M. Kranenburg,[†] Hanneke M. L. Thijs,[†] Renzo M. Paulus,[†] Bart M. van Lankvelt,[†] Jos de Hullu,[†] Menno Springintveld,[†] Davin J. G. Thielen,[†] Catherine A. Tweedie,[‡] Richard Hoogenboom,[†] Krystyn J. Van Vliet,[‡] and Ulrich S. Schubert*[,†,§]

Laboratory of Macromolecular Chemistry and Nanoscience, Eindhoven University of Technology and Dutch Polymer Institute (DPI), P.O. Box 513, 5600 MB Eindhoven, The Netherlands; Laboratory for Material Chemomechanics, Massachusetts Institute of Technology, 77 Massachusetts Avenue, Cambridge, Massachusetts; and Laboratory of Organic and Macromolecular Chemistry, Friedrich-Schiller-University Jena, 07743 Jena, Germany

Received March 24, 2007; Revised Manuscript Received June 7, 2007

ABSTRACT: The purpose of this study was to synthesize copolymers of different molecular architecture, i.e., monomer distribution over the polymer chain, and to compare their physical and mechanical properties. A series of random copolymers of 2-ethyl-2-oxazoline (EtOx) and 2-nonyl-2-oxazoline (NonOx) were synthesized via a cationic ring-opening polymerization procedure in acetonitrile under microwave irradiation. The polymerization kinetics for EtOx and NonOx were studied in refluxing butyronitrile using thermal heating. The resulting kinetic data were applied to synthesize a series of block copolymers with the same chemical composition as the random copolymers. The random and block copolymers exhibited the desired composition, molecular weight, and narrow molecular weight distribution. The surface energies of the random copolymers with 65−85 wt % NonOx were higher than the surface energy of their block copolymer counterparts as the random distribution of EtOx units hindered the segregation of the NonOx units to the surface. The variation in polymer architecture also resulted in different phase segregation behavior and different transition temperatures, as shown by differential scanning calorimetry (DSC). The observed elastic moduli, which differed considerably between the random and the block series, were well explained by the phases identified through DSC.

1. Introduction

The living nature of the cationic ring-opening polymerization (CROP) of 2-substituted-2-oxazolines, discovered in 1966,[1−4] allows facile preparation of well-defined (co)polymers, including amphiphilic copolymers.[5] The CROP can be initiated by a strong electrophile (here, methyl tosylate) that is attacked by the endocyclic nitrogen of the 2-substituted-2-oxazoline to form an oxazolinium ring (Scheme 1).[6−8] The C−O bond of this cationic ring is weakened, and propagation occurs by the nucleophilic attack of the next monomer on this carbon atom. After all the monomer is consumed and the reaction is complete, a second monomer can be added to form a block copolymer or the polymerization can be terminated by the addition of a nucleophile (e.g., water).

Depending on the utilized monomers, the properties of the resulting poly(2-oxazolines) can be easily varied. Methyl and ethyl side groups result in water-soluble polymers, whereas longer alkyl or aromatic groups result in hydrophobic polymers.[9,10] The combination of such monomers in one polymer chain provides facile synthesis of amphiphilic copolymers,[11] which are then amenable to applications such as micellar catalysis, drug delivery, and biomimicking hydrogels.[7−15] It is known that, in general, the monomer distribution can have a significant influence on the properties of the polymers.[16,17] Cai and Litt described the synthesis and several structure−property relationships (regarding properties such as glass transition, melting point, surface energy, crystallographic data, adhesion, etc.) of random and some block copoly(oxazoline)s with various side groups.[18−21] In the current work, we report the synthesis and structure−property relationships for copolymers of 2-ethyl-2-oxazoline (EtOx) and 2-nonyl-2-oxazoline (NonOx), a system not yet discussed in the literature. Furthermore, a direct comparison between the properties of both the random and the block architecture is made at EtOx:NonOx compositions systematically varied from p(EtOx) to p(NonOx). The block copolymers were synthesized under reflux temperature using conventional heating, whereas the random copolymers were synthesized using microwave heating.[22] For the polymerization of block copolymers, butyronitrile was used as solvent. This is a less common solvent, and therefore the kinetics of this system were investigated before the block copolymerizations were performed. Surface energies of the synthesized copolymers were determined using contact angle measurements, and thermal transitions were measured via differential scanning calorimetry (DSC). The presence of crystalline or amorphous phases, as indicated by DSC, was related to the elastic modulus of each copolymer obtained from depth-sensing indentation. The distribution of the monomer units along the polymer chain significantly affected the observed physical and mechanical properties. Both the synthesis and screening of the libraries of random and block copoly(2-oxazoline)s were performed using a high-throughput workflow, demonstrating the power to screen and optimize polymer properties as well as to gain fundamental understanding of structure−property relationships in polymer science.

* Corresponding author: Fax (+31) 40 247 4186; e-mail u.s.schubert@tue.nl.
[†] Eindhoven University of Technology and Dutch Polymer Institute.
[‡] Massachusetts Institute of Technology.
[§] Friedrich-Schiller-University Jena.

10.1021/ma070720r CCC: $37.00
Published on Web 07/10/2007

Scheme 1. Schematic Representation of the Living Cationic Ring-Opening Polymerization of 2-Substituted 2-Oxazolines, Initiated by Methyl Tosylate

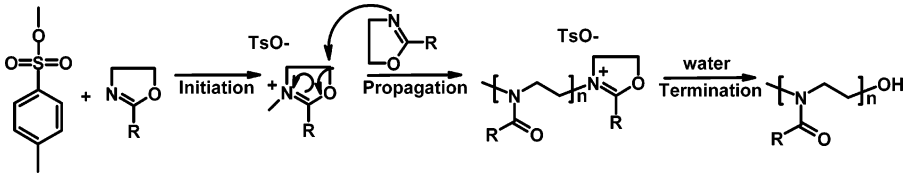

2. Experimental Section

2.1. Synthesis. 2-Ethyl-2-oxazoline (EtOx, Aldrich), 2-nonyl-2-oxazoline (NonOx, Henkel), and methyl tosylate (MeOTs, Aldrich) were distilled and stored under argon. Acetonitrile (ACN, Biosolve Ltd.) and butyronitrile (BCN, Aldrich) were dried over molecular sieves (3 Å). Kinetic studies as well as the block copolymerizations were performed on a Chemspeed ASW2000 automated synthesizer with a reactor block with 16 reaction vessels of 13 mL. These reaction vessels were equipped with a heating jacket connected to a Huber Unistat 390 W cryostat (−90 to 150 °C). All reaction vessels were equipped with coldfinger reflux condensers that could be controlled from −5 to 45 °C. Agitation of the reaction mixture is performed by a vortex movement of the reactors. An inert atmosphere was maintained by applying a 1.1 bar argon flow over the reaction vessels and a 1.5 bar argon flow through the hood of the automated synthesizer. Random copolymerizations were performed in capped reaction vials uniquely designed for the single-mode microwave system Emrys Liberator (Biotage). These vials were heated and cooled under argon before filling with chemicals. The polymerizations were quenched by the addition of water.

Kinetic Investigation of Homopolymers. The inert atmosphere in the hood of the Chemspeed ASW2000 was obtained by flushing with argon for at least 45 min. Before the reactions were started, the reaction vessels were heated to 120 °C, evacuated for 15 min, and subsequently filled with argon. This procedure was repeated three times to create an inert atmosphere in the reaction vessels. Pure 2-oxazoline and stock solutions of methyl tosylate were transferred into the 13 mL reaction vessels, resulting in 4 M concentration of monomer for 2-ethyl-2-oxazoline and in 2 M for 2-nonyl-2-oxazoline with a monomer-to-initiator ratio of 60. The mixtures were heated up to 130 °C under vortexing at 600 rpm for ∼40 min with the reflux condensers set at −5 °C. During the reaction time, samples were automatically transferred to 2 mL vials prefilled with chloroform saturated with water at suitable time intervals.

Random Copolymerizations. Microwave vials were heated at 105 °C for at least 2 h and cooled down under an argon atmosphere. The ASW2000 automated synthesizer (flushed with argon for 1 h) performed filling of these vials. Pure monomers (varying amounts) and a stock solution of methyl tosylate (14.9 mg, 0.08 mmol) in 423 μL of acetonitrile were transferred into the microwave vials, resulting in a total 2-oxazoline concentration of 4 M. The monomer-to-initiator ratio was kept constant at 100, and the total reaction volume was 2 mL. The vials were capped and mixed and samples were automatically transferred to GC vials prefilled with chloroform saturated with water. The polymerization mixtures were heated to 140 °C using the single-mode microwave system Emrys Liberator (Biotage). For the random copolymers two different reaction times were performed: one to full conversion (reaction time of 600 s) and one where only a part of the monomer reacted to determine the reactivity ratios (reaction time of 180 s). After the reaction was finished the polymerizations were terminated by addition of water.

Block Copolymerizations. Block copolymers were synthesized in a similar manner as described for the kinetic investigations of the homopolymers using a total monomer-to-initiator ratio of 100, whereby the first block was synthesized, and after a predefined time, a second monomer was added from a stock solution (varying amounts) to prepare the block copolymers.

2.2. Characterization Techniques. Size exclusion chromatography (GPC) was measured on a Shimadzu system equipped with a SCK-10A system controller, a LC-10AD pump, a RID-10A refractive index detector, and a PL gel 5 μm Mixed-D column at 50 °C utilizing a chloroform:triethylamine:isopropanol (94:4:2) mixture as eluent at a flow rate of 1 mL min^{-1}. The molecular weights were calculated against polystyrene standards. Gas chromatography (GC) measurements were performed on an Interscience Trace GC equipped with a PAL autosampler, a special liner, and a Trace Column RTX-5. ^{1}H NMR spectra were recorded on a Varian Mercury 400 spectrometer using deuterated $CHCl_3$.

Contact angle measurements were performed on polymer films prepared by spin-coating of chloroform solutions (20 mg/mL) of the polymer on precleaned microscopy slides at 1000 rpm for 90 s using a WS-400/500 series spin-coater from Laurell Technologies Corp. An automated OCA30 optical contact angle measuring instrument from Dataphysics was used to determine the contact angles of both diiodomethane and ethylene glycol as apolar and polar test liquids, respectively, using the equation-of-state theory to calculate the surface energy (SE).[23]

Thermal transitions were determined on a DSC 204 F1 Phoenix by Netzsch under a nitrogen atmosphere from −100 to 170 °C with a heating rate of 40 K min^{-1} for the glass transition temperature and a heating rate of 10 K min^{-1} for the melting temperature. (The first heating run to 170 °C, which was followed by a cooling run at 40 K min^{-1}, was not considered for the subsequent calculations.) For p(EtOx$_{60}$-*r*-NonOx$_{40}$), p(EtOx$_{50}$-*r*-NonOx$_{50}$), and p(EtOx$_{40}$-*r*-NonOx$_{60}$), DSC measurements were repeated with an annealing period before the last heating step in the DSC measurement program to provoke crystallization. The annealing was performed at 40 °C for 24 h for p(EtOx$_{60}$-*r*-NonOx$_{40}$) and p(EtOx$_{50}$-*r*-NonOx$_{50}$) and for 10 min (preceded by slow unassisted cooling from 200 to 40 °C) for p(EtOx$_{40}$-*r*-NonOx$_{60}$).

The elastic moduli of the materials were characterized via depth-sensing indentation (DSI) on spots of the copoly(oxazoline) materials, drop-cast from a solution of the polymer in chloroform.[24] These polymer films were dried for 3 weeks at ambient humidity and another 3 weeks at 40 °C in vacuum. DSI was conducted at 5.4 ± 0.4% relative humidity (RH) using a TriboIndenter (Hysitron Inc., Minneapolis, MN) with a NanoDMA06 transducer equipped with a diamond Berkovich (three-sided pyramid) indenter. For quasi-static testing, a 10 s loading, 10 s hold at maximum load, and 2 s unloading profile were applied, and the reduced modulus E_r was determined from the unloading response.[24−26] Measurements were repeated at eight maximum loads, decreasing in steps of 300 μN from 2400 to 300 μN. The first two replicates of each experiment were not analyzed to minimize effects of thermal drift. From the reduced modulus E_r, the indentation modulus E_i was calculated using the elastic modulus and Poisson's ratio of the diamond indenter, 1100 GPa and 0.07, respectively, and a Poisson's ratio of 0.4 for the polymeric material.[25,26] The E_i of polymers slightly exceeds the value of E obtained by uniaxial tension due to several factors including high strains relative to the elastic limit, superposed hydrostatic stress, and assumptions of contact at the indent perimeter.[24,27] Storage moduli E' and loss tangent tan δ were determined using the TriboIndenter nanoDMA (nanodynamic mechanical analysis) module, whereby an oscillating load (nominally 10 μN, frequency 20 Hz) was superimposed over the quasi-static load (nominally 300 μN). The storage modulus E' and tan δ are calculated from the ratio and the phase lag between the applied load oscillation and the resulting displacement oscillation.[28−30] The latter was between 0.9 and 4.5 nm in amplitude. The presented storage moduli E' have been converted from "reduced" to "indenta-

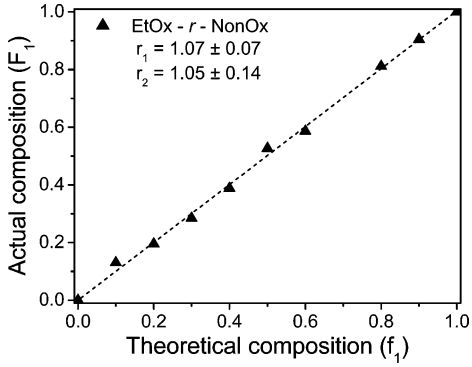

Figure 1. Relation between the fraction of EtOx in the monomer feed (f_1) and the incorporated fraction of EtOx in the random copolymer (F_1) at ~50% conversion. The reactivity ratios are determined utilizing nonlinear least-squares fitting of the data.

tion" storage moduli via the same procedure as described above for the quasi-static results. Five experiments were conducted on both duplicate samples of one copolymer material; the first two were disregarded to minimize effects of thermal drift, and the average and standard deviation out of the six remaining measurements are reported.

3. Results and Discussion

3.1. Random Copolymerizations. A systematic series of statistical copolymers consisting of EtOx and NonOx were synthesized by varying the monomer feeds. The polymerizations were performed in acetonitrile at 140 °C under microwave irradiation with a total monomer concentration of 4 M and a [M]/[I] ratio of 100. The polymerization mixtures were automatically prepared in an ASW2000 synthesis robot as reported previously.[31] Polymerization mixtures with 0−100 mol % (in increments of 10 mol %) of NonOx were prepared and polymerized to full conversion in 10 min at 140 °C under microwave irradiation according to a kinetic study previously reported.[32] In addition, a second series of the same reaction mixtures was prepared and polymerized for 3 min up to half conversion to determine the reactivity ratios of the copolymerizations. For living polymerizations, the reactivity ratios should be calculated at monomer conversions of 20% or higher because the monomer reactivities during initiation may differ from the monomer reactivities during propagation of the polymerization reaction;[33,34] also, for the CROP of 2-substituted-2-oxazolines the polymerization rate during initiation differs from the propagation rate.[35,36] The incorporated monomer fractions (F_1) at half conversion (determined by ^{1}H NMR spectroscopy) are plotted against the theoretical composition (f_1) in Figure 1. The reactivity ratios for the statistical copolymerization of EtOx and NonOx were determined utilizing nonlinear least-square fitting of the data shown in Figure 1[37] and were equal to unity within the standard deviation (Figure 1), indicating the formation of truly random copolymers. Similar reactivity ratios were also reported in the literature for the copolymerization of EtOx and NonOx using benzyl bromide as initiator and *N*,*N*-dimethylacetamide as solvent at 100 °C with thermal heating.[38] The copolymerizations that were carried out aiming for full conversion yielded copolymers with the desired compositions (determined by ^{1}H NMR spectroscopy; not shown). Size exclusion chromatography (SEC) of the copolymers revealed monomodal molecular weight distributions with polydispersity indices (PDI) below 1.20 (except p(EtOx$_{10}$-*r*-NonOx$_{90}$), PDI = 1.34), indicating good control over the polymerization reactions (Figure 2). In addition, the number-average molecular weight (M_n) increased with increasing mole fraction of NonOx because of the higher

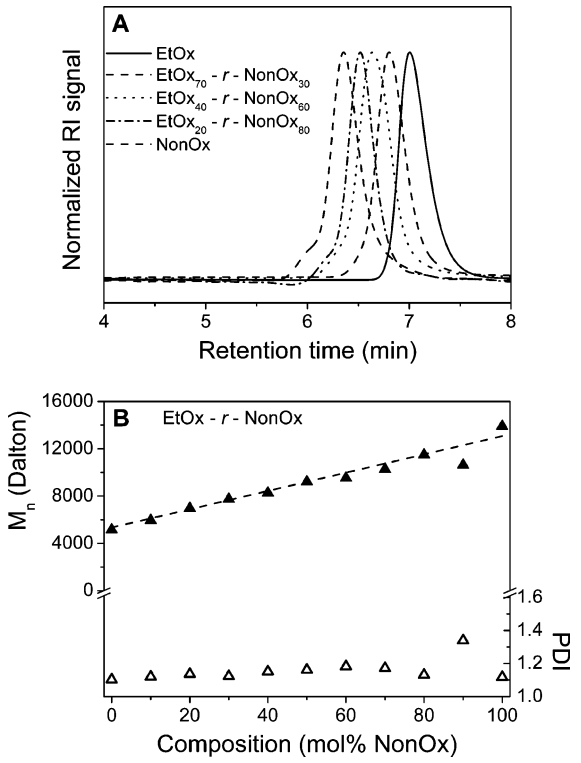

Figure 2. (A) Selected SEC traces of EtOx-*r*-NonOx copolymers with different amounts of NonOx content (SEC eluent: $CHCl_3$ with 2% isopropanol and 4% triethylamine). (B) M_n and PDI values of the EtOx-*r*-NonOx copolymers resulting from SEC analysis.

molecular weight of this monomer and the constant monomer: initiator ratio of 100. However, it should be noted that the calculated M_n's are lower than the theoretical M_n's, which can be ascribed to the used calibration (PS standards).

3.2. Block Copolymerizations. Whereas the EtOx−NonOx random copolymerizations were synthesized using pressurized microwave conditions, the sequential block copolymerizations were performed under reflux with thermal heating to simplify the addition of the second monomer. The polymerization solvent was changed from acetonitrile (boiling point 82 °C) to butyronitrile (boiling point 115−117 °C) to allow a higher reaction temperature (and thus accelerated polymerization) when working under reflux conditions.

Prior to the synthesis of block copolymers in butyronitrile, the kinetics of the homopolymerizations were investigated in refluxing butyronitrile to identify the required optimal polymerization times. These kinetic investigations were performed in an automated Chemspeed ASW2000 synthesis robot.[39] EtOx and NonOx polymerization mixtures were prepared in butyronitrile with methyl tosylate as initiator, 4 M monomer concentration for EtOx, and 2 M monomer concentration for NonOx using a monomer-to-initiator ratio of 60. These polymerization mixtures were heated to reflux (set temperature of 130 °C), and samples were automatically transferred to 2 mL vials at suitable time intervals to investigate the polymerization kinetics. The samples were analyzed by gas chromatography (GC) and SEC to determine the monomer conversions as well as the molecular weight (distributions), respectively. The resulting first-order kinetic plot and M_n as a function of conversion are shown in Figure 3. The first-order kinetic plot (Figure 3A) is linear for both monomers, demonstrating a constant concentration of propagating species during the polymerizations. The slope of the first-order kinetic plot for the NonOx polymerization at 2 M ([MeOts] = 0.033 M) is half

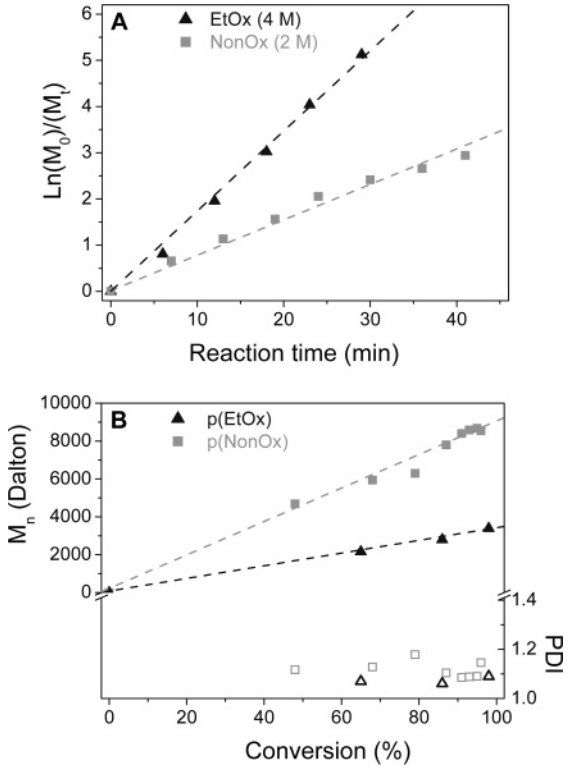

Figure 3. (A) Reaction kinetics (GC) obtained from automated screening of the 2-ethyl- and 2-nonyl-2-oxazoline polymerization in refluxing butyronitrile ([M]/[I] = 60, methyl tosylate as initiator). (B) M_n against conversion plot for the kinetic screening of the 2-ethyl- and 2-nonyl-2-oxazoline polymerization in butyronitrile.

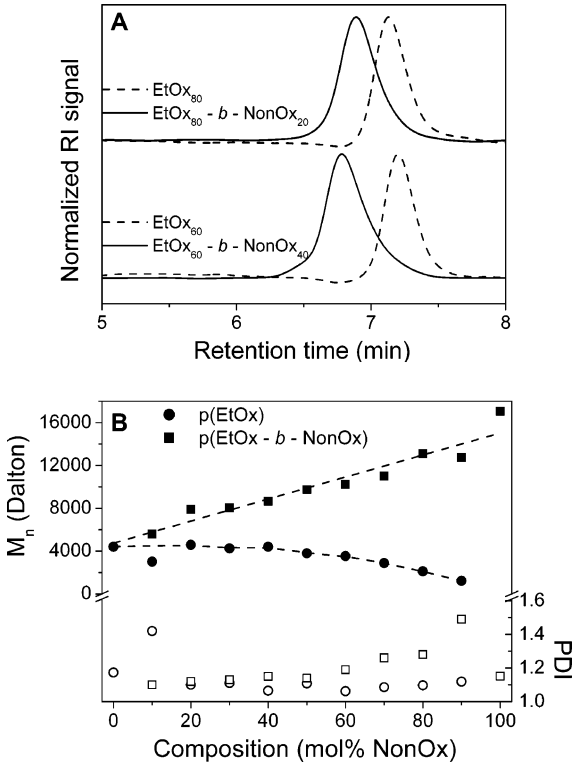

Figure 4. (A) Selected SEC traces of the EtOx polymers (first block) and the corresponding EtOx-*b*-NonOx copolymers with different amounts of NonOx content (SEC eluent: $CHCl_3$ with 2% isopropanol and 4% triethylamine). (B) M_n and PDI values of the EtOx-*b*-NonOx copolymers resulting from SEC analysis.

the slope of the first-order kinetic plot for the EtOx polymerization at 4 M ([MeOTs] = 0.066 M), indicating that the polymerization rate for both monomers is similar. The linear increase of number-averaged molecular weight (M_n) with conversion and the corresponding low PDIs further demonstrate the living nature of the polymerization of both monomers in butyronitrile (Figure 3B).

On the basis of the determined polymerization kinetics, the polymerization times required for the synthesis of the EtOx:NonOx block copolymers in refluxing butyronitrile were calculated. The monomer compositions of the block copolymers were similar to that of the random copolymers (ranging from 0 to 100% NonOx in increments of 10 mol %), having a total degree of polymerization of 100. The EtOx:NonOx block copolymers were synthesized in an ASW2000 automated synthesizer using a sequential monomer addition procedure, whereby the EtOx was used for the first block and NonOx was added as second block. After the polymerization of monomer EtOx (4 M monomer concentration) for a predefined reaction time, a sample was taken from the reaction mixtures to analyze the first block. Subsequently, neat NonOx was added into the reactor and the polymerization was continued. The end samples were analyzed by SEC and ^{1}H NMR spectroscopy. Selected SEC traces of some first blocks and the corresponding block copolymers are shown in Figure 4A, demonstrating the successful block copolymerizations. Figure 4B depicts the SEC results obtained for the first blocks and the final block copolymers demonstrating that the M_n of the first blocks decreased with increasing NonOx content and the final M_n's increased. Furthermore, the first blocks and the block copolymers revealed polydispersity indices below 1.2 (except for the aimed combination of p(EtOx$_{90}$-*b*-NonOx$_{10}$), PDI $_{\text{block A}}$ = 1.44), indicating good control over the polymerizations. ^{1}H NMR spectroscopy indicated that all EtOx:NonOx block copolymers consisted of the desired compositions except for p(EtOx$_{90}$-*b*-NonOx$_{10}$) (Figure 5). Since the p(EtOx$_{90}$-*b*-NonOx$_{10}$) copolymer does not have the desired composition and exhibits an unexpectedly broad molecular weight distribution, this polymer is excluded from further discussion.

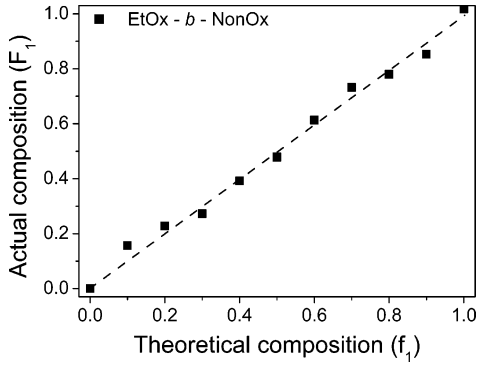

Figure 5. Actual composition plotted against theoretical composition, measured by ^{1}H NMR for the EtOx-*b*-NonOx copolymers.

3.3. Surface Energies of the Synthesized Copoly(2-oxazoline) Series. The surface energies (SE) were investigated for the two successfully synthesized copolymer series by contact angle measurements[23] of two different test liquids on spin-coated polymer films. Since p(NonOx) has a surface energy of ~22 mN m^{-1} and p(EtOx) around 45 mN m^{-1}, the SE should range between these two values throughout the copolymer series.[40] Figure 6 shows the determined surface energies for the EtOx:NonOx random and block copolymer series as a function of chemical composition. The random copolymers exhibited a slight decrease in SE up to 70 wt % of incorporated NonOx. Above 70 wt % NonOx, the SE decreases gradually to 22 mN

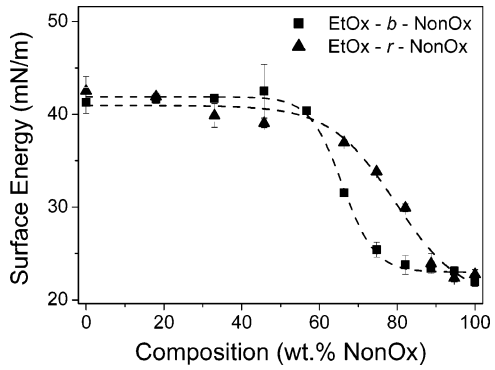

Figure 6. Surface energies calculated from the contact angles of diiodomethane and ethylene glycol for the random and block EtOx-NonOx copolymers. A sigmoidal fit is used to fit the data.

m^{-1}, which is ascribed to a sufficient NonOx content to cover the majority of the surface with nonyl side chains by preferential orientation. Nonetheless, the random incorporation of EtOx prevents complete surface coverage by NonOx, which explains the gradual decrease in SE. In contrast, the SE of the block copolymers is constant at ~42 mN m^{-1} up to 60 wt % NonOx, while increasing the NonOx content further results in a sharp decrease of SE to 22 mN m^{-1}. The nonyl side chains in the block copolymers can, compared to the nonyl side chains in the random copolymers, cover the surface more easily. Annealing of both copolymer series at 80 °C for 20 h resulted in slightly lower SE's (results not shown) but exhibited the same trends as before annealing.

3.4. Thermal Transitions of the Synthesized Copoly(2-oxazoline) Series. The thermal transitions of the two copolymer materials were investigated by differential scanning calorimetry (DSC); a melting peak in the DSC reveals the presence of crystalline regions (at temperatures below the melting transition), while a glass transition reveals the presence of amorphous regions. The determined melting temperature (T_m) and glass transition temperature (T_g) of the synthesized copolymers are depicted in Figure 7.

The T_g of p(NonOx) is lower than the T_g of p(EtOx).[40] Therefore, for the EtOx:NonOx random copolymers the T_g is reduced with increasing amount of NonOx. In contrast, the T_g's of the block copolymers containing 33−82 wt % NonOx is close to the T_g of pure p(EtOx): as a large fraction, or all, of the NonOx segregates into a NonOx-rich (semi)crystalline phase, the glassy phase does not contain as much NonOx as for the random series.

At higher amounts (≥82 wt %) of NonOx, the random copolymer material also comprises a crystalline phase, with a melting temperature that is considerably lower than for the pure NonOx. With increasing NonOx content, both T_m and the melting enthalpy (not shown) increase, as less EtOx side chains disturb the crystallization.[41] For the block copolymer series, the melting enthalpy increased with increasing NonOx content, as the volume fraction of the crystalline phase increases with increasing NonOx content.

For the p($EtOx_{60}$-*r*-$NonOx_{40}$), p($EtOx_{50}$-*r*-$NonOx_{50}$), and p($EtOx_{40}$-*r*-$NonOx_{60}$), NonOx content of 57, 67, and 75 wt %, respectively, DSC measurements were repeated with an annealing period before the last heating step in the DSC measurement program. As the annealing temperature (40 °C) is above the T_g of these materials, appreciable polymer chain segmental motion is possible and can facilitate crystallization. No melting peak was observed for p($EtOx_{60}$-*r*-$NonOx_{40}$) after 24 h annealing at 40 °C, indicating that this material remains amorphous. After annealing p($EtOx_{50}$-*r*-$NonOx_{50}$) and p($EtOx_{40}$-*r*-$NonOx_{60}$), a melting peak was observed that was not measured without annealing, indicating that a crystalline phase was nucleated upon annealing.

The phases expected to be present at room temperature, based on the DSC results, are summarized in Table 1. The crystalline phases will be richer in NonOx than the amorphous phase but may contain some EtOx as well. Similarly, the amorphous phases may contain some NonOx. In Table 1, the pure p(NonOx) is described as "crystalline", though this polymer may be either fully crystalline or semicrystalline: it may contain amorphous regions that comprise a too small volume fraction to detect via the DSC heat flow.

In view of the mechanical properties that will be discussed later, Table 1 distinguishes between amorphous material that is, when probed at room temperature, below T_g (i.e., glassy) and amorphous material that is at room temperature above T_g. Although these two phases are thermodynamically similar,[41] their mechanical behavior is very different as described in the next section.

3.5. Mechanical Properties of the Synthesized Copoly(2-oxazoline) Materials. Although all polymers are viscoelastic and thus exhibit mechanical properties that depend on time and temperature,[41,42] glassy polymers (i.e., amorphous polymers characterized below T_g) generally exhibit an effective Young's elastic modulus E (via uniaxial tension) or storage modulus E' (via dynamic mechanical analysis) of approximately 2.5−4.5 GPa.[41] As testing temperature approaches T_g, E and E' gradually decrease; above T_g, the thermal energy of the polymeric chains is large enough that segments of the polymer chain can overcome the secondary bonding among chains, resulting in appreciable segmental mobility and in an elastic modulus below 100 MPa for amorphous materials. The exact temperature range over which the mechanical behavior changes from the glassy

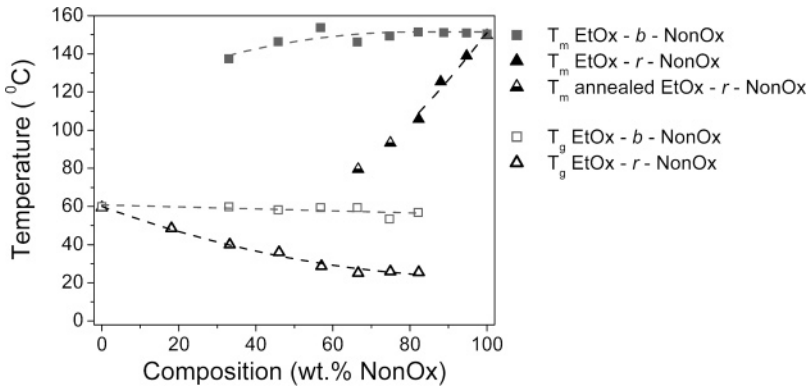

Figure 7. Glass transition temperatures and melting temperatures for the random and block EtOx:NonOx copolymers.

Table 1. Phases Expected To Be Present at 25 °C for the Studied Compositions Based on the DSC Data Shown in Figure 7[a]

composition, wt % (mol %) NonOx	0 (0)	18 (10)	33−57 (20−40)	66−82(50−70)	88−100 (80−100)
block series	glassy	disregarded[b]	crystalline + glassy	crystalline + glassy	crystalline
random series	glassy (amorphous with T_g > 25 °C)		amorphous above or below T_g	crystalline + amorphous above or below T_g	crystalline

[a] Materials are listed as containing a crystalline phase if their DSC trace exhibited a melting peak after annealing at 40 °C for durations up to 24 h or already after no annealing at all. [b] One sample is not included in the table as the SEC and ^{1}H NMR showed that it did not possess the chemical characteristics aimed for.

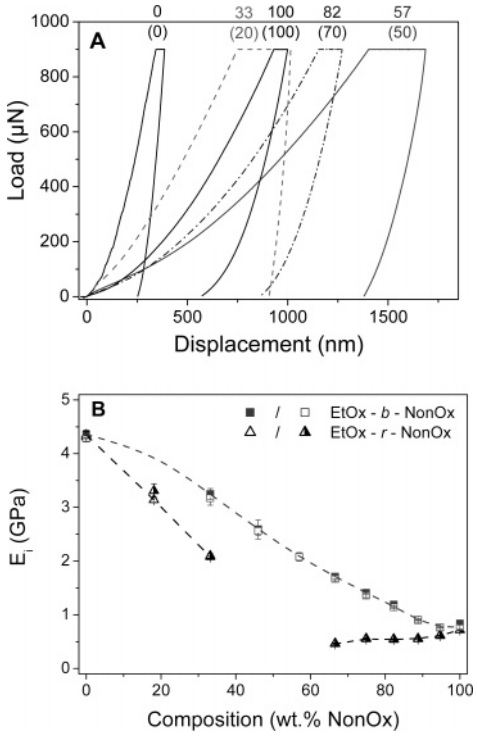

Figure 8. (A) Selected load−displacement responses for the EtOx-*r*-NonOx copolymers at 5.4% RH; wt % (mol %) NonOx are indicated for each response. (B) E_i resulting from analysis of up to six load−displacement responses.

to rubbery response depends on the method and time scale of mechanical testing.[41,42] For semicrystalline materials, the elastic modulus drops at T_g to approximately 0.5−1.0 GPa, the exact value depending on the degree of crystallinity.[41]

Typical load−displacement responses as measured via depth-sensing indentation (DSI) at 5.4% relative humidity (RH) are shown in Figure 8A. Pure p(EtOx) was more resistant to contact loading than pure p(NonOx), in that p(EtOx) exhibited a smaller depth of penetration when loaded up to the same maximum applied load. Additionally, the creep compliance of random copolymers with intermediate NonOx content (e.g., 57 wt % NonOx in Figure 8A) was considerable, as indicated by large displacement of the indenter at constant, maximum applied load; this appreciable creep complicated the inference of elastic properties from DSI but qualitatively indicated lower resistance to deformation over the time scale of the DSI experiment (loading in 10 s and 10 s hold time at maximum load) compared to pure p(EtOx) or p(NonOx).

The indentation moduli E_i obtained from the analysis of these load−displacement responses are shown in Figure 8B. $E_i = 4.3$ GPa was found for p(EtOx), a typical value for the E_i of a glassy polymer. E_i of p(NonOx) is ∼0.8 GPa (Table 2). This higher stiffness than typically measured for a polymer probed at a temperature above its T_g is due to the crystallinity of this material.[24] At intermediate compositions, the EtOx:NonOx copolymer materials with a block architecture exhibited a higher stiffness than the random copolymers with corresponding compositions (Figure 8B). This is caused by the higher degree of crystallinity and the larger difference between their T_g's and the testing temperature (room temperature) of the block copolymers compared to the random copolymers (Table 1 and Figure 7), as discussed in more detail throughout this section.

Table 2. Comparison of the Reduced Moduli E_r for All Materials That Had a Corresponding Counterpart in a Previous Work[24]

current work			previous work	
sample name	E_i[a] (GPa)	E_r (GPa)	sample name	E_r (GPa)
p(EtOx) random series	4.3	5.1	EtEt	5.1
p(EtOx) block series	4.3	5.1		
p(NonOx) random series	0.72	0.86	NonNon	1.0
p(NonOx) block series	0.80	0.96		
p($EtOx_{50}$-*b*-$NonOx_{50}$)	1.7	2.0	EtNon	2.1

[a] The indentation moduli E_i are calculated from the reduced moduli E_r as described in the Experimental Section.

The obtained elastic moduli obtained via DSI for the homopolymers and the block copolymer with 50 mol % NonOx agree well with previously reported results for polymeric materials of identical chemical composition and chain length (Table 2).[24] The variation in E_r, which may be due to differences in synthesis conditions (e.g., polymerization was conducted in another solvent for the random series compared to the block series) and batch-to-batch and operator variability, was only small. The sample codes that were used in the previous work are included for easy comparison. (Presented data for each series were obtained on two duplicate drop-cast samples. Standard deviations, omitted in Table 2, can be found in the graphics and are typically 0.05 GPa.)

The random copolymers with 18 and 33 wt % NonOx exhibited a lower E_i than pure p(EtOx). At room temperature, these materials are still below their T_g, but the difference between their glass transition temperatures and room temperature is smaller than for p(EtOx). Because of the hygroscopic nature of p(EtOx), this difference will be even smaller than the ∼25 and ∼15 °C, respectively, indicated in Figure 7. Traditional mechanical testing of bulk amorphous polymers shows that the change in the elastic modulus at the glass transition occurs gradually.[41−43] Thus, the decreased E_i of these random copolymers with respect to pure p(EtOx) is not unexpected.

For the random copolymers with 46 and 57 wt % NonOx, E_i could not be determined using quasi-static DSI. The quasi-static analysis assumes predominantly elastic material behavior upon initial decrease of the load on the indenter.[26,27,30] For those two random copolymers, this was clearly not the case: upon unloading, the probe initially continued to displace into the material (46 wt % NonOx) or remained at the same depth (57 wt % NonOx) due to the appreciable creep. The creep compliance of these two materials was large compared to glassy or semicrystalline polymeric materials.[44] In addition, all measurements on these materials (46 wt % NonOx) or all but one

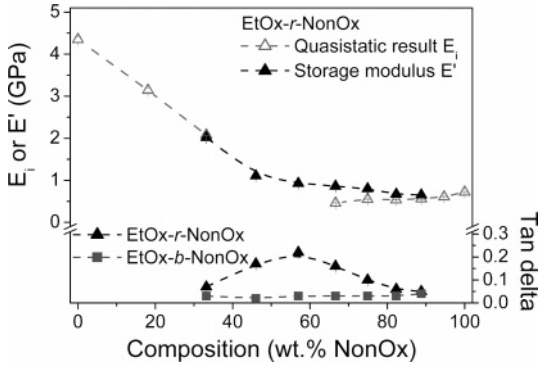

Figure 9. Storage modulus E' (random series only) and loss tangent tan δ (random and block series) obtained by dynamic indentation (5.6 ± 0.4 % RH); quasi-static E_i results are included for comparison.

(57 wt % NonOx) were outside the depth range of the calibrated probe area function that was employed to determine E_i from DSI experiments. The large time-dependent deformation for materials that are close to T_g when probed at room temperature is attributed to the chain length: the poly(oxazoline)s discussed in this study are only 100 monomer units long (see Scheme 1 for the structure of the units), which results in only a small number of entanglements per polymer chain.[45] The moduli displayed in Figure 8B for the random copolymers with 33, 67, and 75 wt % NonOx should be treated with circumspection, as creep somewhat affected the analysis accuracy.[46]

We note that, prior to DSI, all samples were dried for 3 weeks at 40 °C to remove the solvent used during deposition of the polymer spots. During this drying, crystallization could occur. This crystallization reduced the time-dependent deformation of the random EtOx:NonOx copolymers with 75 and 67 wt % NonOx, so that the material behavior upon unloading was predominantly elastic and E_i could be obtained. However, only little or no crystallization occurred for the random copolymers with 57 and 46 wt % NonOx. The hypothesized low degree, or even absence, of crystallinity for these materials is supported by the absence of any observable melting peak in the DSC trace after 24 h annealing for the random copolymer containing 57 wt % NonOx (Figure 7). As their T_g was close to room temperature and only little or no crystallization had taken place, the time-dependent deformation of the random copolymers with 57 and 46 wt % NonOx was too large to determine E_i robustly.

For block copolymers with a composition between the pure glassy phase and the pure crystalline phase, E_i is expected to be a volume-weighted average of the modulus of the glassy phase and the crystalline phase.[43] With increasing NonOx content, the volume fraction of the crystalline phase will be increased, and thus the block copolymer elastic properties will increasingly reflect those of the pure crystalline phase. Indeed, E_i gradually (and almost linearly) decreased from that typical for the glassy phase (~4.4 GPa) to that typical for the crystalline phase (~0.8 GPa). In conclusion, at intermediate composition the copolymer material with block architecture exhibited stiffer material response than the random architecture, as the block copolymer material has a higher degree of crystallinity and a higher T_g than the random copolymer material (N.B.: for systems based on other monomer units, the degree of crystallinity may have the opposite effect on the stiffness compared to the current study).[41]

The relative storage moduli E' and loss tangents tan δ determined by dynamic indentations are presented for the random copolymers in Figure 9. For two random copolymer materials in Figure 8B, the time-dependent plastic or very slow viscoelastic response to the load impeded the determination of E_i from the quasi-static DSI experiments, but dynamic indentation, which probes the reversible (viscoelastic) response to a small contact load oscillation (here, at a frequency of 20 Hz), was performed succesfully. E' exhibited a gradual decrease with increasing NonOx content. For the random copolymers with up to 57 wt % NonOx, tan δ increased with increasing NonOx content; at 57 wt % NonOx, the majority of the energy produced by the probe oscillation was dissipated, presumably as heat. Large heat dissipation relative to the elastically stored energy is typical for a material that is close to its T_g.[41] When the NonOx content increased even further, tan δ decreased. The difference between the storage modulus E' at 20 Hz and the quasi-static modulus E_i decreased as well (Figure 9). We conclude that the decrease in tan δ, which indicates a smaller viscous component in the viscoelastic material response, was caused by the increase in the degree of crystallinity upon increasing NonOx content.

The E' of the block copolymers (not shown) exhibited the same decrease with increasing NonOx content as did the quasi-static moduli E_i. At intermediate compositions, the block copolymer materials were probed at a temperature well below their T_g and contained a larger crystalline volume fraction than their random copolymer counterparts. Therefore, tan δ at intermediate NonOx contents is lower for the block architecture than for the random architecture (Figure 9).

4. Conclusions

We have demonstrated the successful synthesis of random EtOx:NonOx copolymers under microwave irradiation. In addition, the reactivity ratios were determined revealing the formation of random EtOx:NonOx copolymers. Furthermore, the kinetics of EtOx and NonOx polymerizations in refluxing butyronitrile with conventional heating were investigated. This kinetic study was used as basis for the synthesis of well-defined EtOx:NonOx block copolymers with similar monomer compositions as the corresponding random copolymers. SEC and ^{1}H NMR spectroscopy showed that the random and (nearly all of) the block copolymers exhibited the desired chemical composition, molecular weight, and narrow molecular weight distribution.

Contact angle measurements and the corresponding calculated surface energies showed that the block copolymer organization results in a more effective NonOx enrichment at the surface and therefore a pronounced decrease in the surface energy at a critical NonOx content (~65 wt % NonOx), whereas the transition is more gradual for the random organization. The monomer distribution along the copolymer chains significantly affected both the nature of the phases present and their transition temperatures. The volume fractions of the amorphous and the crystalline phases as well as the location of the glass transition temperature with respect to room temperature governed the mechanical properties. For random copolymers with intermediate EtOx:NonOx composition, the EtOx units disturb the crystallization; further, the long NonOx side chains increase the flexibility in the amorphous phase, thereby decreasing the T_g. This results in a lower degree of crystallinity and a lower T_g (i.e., closer to room temperature) for these random copolymers compared to their block copolymer counterparts. (The NonOx in the block copolymers can segregate more easily into NonOx-rich crystalline regions.) Therefore, random copolymers at intermediate EtOx:NonOx compositions exhibited greater mechanical energy dissipation (higher tan δ), greater creep compliance, and lower elastic moduli E_i than the block copolymers of corresponding composition. Consideration of the thermal history

of the mechanically interrogated samples improved the understanding of the relation between the phases present in the material and the resulting viscoelastic properties. In conclusion, the organization of the monomer units within EtOx:NonOx copolymers has a significant effect on the surface energies, thermal transitions, and mechanical properties of the material, demonstrating that structural control over monomer distributions is an excellent way to tune the physical and mechanical properties of these polymers.

Acknowledgment. This study was supported by the Dutch Polymer Institute (DPI) (projects 401, 496, 500, 502, and 543), the Dutch Scientific Organization (NWO), and the Fonds der Chemischen Industrie. C.A.T. gratefully acknowledges the US National Science Foundation Graduate Fellowship.

References and Notes

(1) Tomalia, D. A.; Sheetz, D. P. *J. Polym. Sci.* **1966**, *4*, 2253−2265.
(2) Seeliger, W.; Aufderhaar, E.; Diepers, W.; Feinauer, R.; Nehring, R.; Thier, W.; Hellmann, H. *Angew. Chem., Int. Ed. Engl.* **1966**, *20*, 913−927.
(3) Kagiya, T.; Narisawa, S.; Maeda, T.; Fukui, K. *Polym. Lett.* **1966**, *4*, 441−445.
(4) Bassiri, T. G.; Levy, A.; Litt, M. *Polym. Lett.* **1967**, *5*, 871−879.
(5) Hoogenboom, R.; Wiesbrock, F.; Huang, H.; Leenen, M. A. M.; Thijs, H. M. L.; van Nispen, S. F. G. M.; van der Loop, M.; Fustin, C.-A.; Jonas, A. M.; Gohy, J.-F.; Schubert, U. S. *Macromolecules* **2006**, *39*, 4719−4725.
(6) Cai, G.; Litt, M. H. *J. Polym. Sci., Part A: Polym. Chem.* **1989**, *27*, 3603−3618.
(7) Saegusa, T.; Ikeda, H. *Macromolecules* **1973**, *6*, 808−811.
(8) Saegusa, T.; Ikeda, H.; Fujii, H. *Macromolecules* **1972**, *5*, 359−362.
(9) Kobayashi, S.; Igarashi, T.; Moriuchi, Y.; Saegusa, T. *Macromolecules* **1986**, *19*, 535−541.
(10) Jin, R. H. *Adv. Mater.* **2002**, *14*, 889−892.
(11) Huang, H.; Hoogenboom, R.; Leenen, M. A. M.; Guillet, P.; Jonas, A. M.; Schubert, U. S.; Gohy, J.-F. *J. Am. Chem. Soc.* **2006**, *128*, 3784−3788.
(12) Aio, K.; Okada, M. *Prog. Polym. Sci.* **1996**, *21*, 151−208.
(13) Jin, R. H. *J. Mater. Chem.* **2004**, *14*, 320−327.
(14) Percec, V.; Bera, T. K.; Butera, R. J. *Biomacromolecules* **2002**, *3*, 272−279.
(15) Chujo, Y.; Sada, K.; Saegusa, T. *Macromolecules* **1993**, *26*, 6315−6319.
(16) Sumi, K.; Anson, F. C. *J. Phys. Chem.* **1986**, *90*, 3845−3850.
(17) Hellmann, G. P.; Dietz, M. *Macromol. Symp.* **2001**, *170*, 1−8.
(18) Cai, G.; Litt, M. H. *J. Polym. Sci., Part A: Polym. Chem.* **1996**, *34*, 2679−2688.
(19) Cai, G.; Litt, M. H. *J. Polym. Sci., Part A: Polym. Chem.* **1996**, *34*, 2689−2699.
(20) Cai, G.; Litt, M. H. *J. Polym. Sci., Part A: Polym. Chem.* **1992**, *30*, 659−669.
(21) Cai, G.; Litt, M. H.; Krieger, I. M. *J. Polym. Sci., Part B: Polym. Phys.* **1991**, *29*, 773−784.
(22) Wiesbrock, F.; Hoogenboom, R.; Abeln, C. A.; Schubert, U. S. *Macromol. Rapid Commun.* **2004**, *25*, 1895−1899.
(23) Wijnans, S.; de Gans, B. J.; Wiesbrock, F.; Hoogenboom, R.; Schubert, U. S. *Macromol. Rapid Commun.* **2004**, *25*, 1958−1962.
(24) Kranenburg, J. M.; Tweedie, C. A.; Hoogenboom, R.; Wiesbrock, F.; Thijs, H. M. L.; Hendriks, C. E.; Van Vliet, K. J.; Schubert, U. S. *J. Mater. Chem.* 2007, in press (DOI: 10.1039/b701945a).
(25) Tweedie, C. A.; Anderson, D. G.; Langer, R.; Van Vliet, K. J. *Adv. Mater.* **2005**, *17*, 2599−2604.
(26) Oliver, W. C.; Pharr, G. M. *J. Mater. Res.* **1992**, *7*, 1564−1583.
(27) Tweedie, C. A.; Van Vliet, K. J. *J. Mater. Res.* **2006**, *21*, 3029−3036.
(28) Syed Asif, S. A.; Wahl, K. J.; Colton, R. J. *Rev. Sci. Instrum.* **1999**, *70*, 2408−2413.
(29) Menčík, J.; Rauchs, G.; Bardon, J.; Riche, A. *J. Mater. Res.* **2005**, *20*, 2660−2669.
(30) Fisher-Cripps, A. C. *Nanoindentation*, 2nd ed.; Springer: New York, 2004.
(31) Hoogenboom, R.; Wiesbrock, F.; Leenen, M. A. M.; Meier, M. A. R.; Schubert, U. S. *J. Comb. Chem.* **2005**, *7*, 10−13.
(32) Wiesbrock, F.; Hoogenboom, R.; Leenen, M. A. M.; Meier, M. A. R.; Schubert, U. S. *Macromolecules* **2005**, *8*, 5025−5034.
(33) Madruga, E. L. *Prog. Polym. Sci.* **2002**, *27*, 1879−1924.
(34) Ziegler, M. J.; Matyjaszewksi, K. *Macromolecules* **2001**, *34*, 415−424.
(35) Saegusa, T.; Kobayashi, S.; Yamada, A. *Makromol. Chem.* **1976**, *177*, 2271−2283.
(36) Hoogenboom, R.; Paulus, R. M.; Fijten, M. W. M.; Schubert, U. S. *J. Polym. Sci., Part A: Polym. Chem.* **2005**, *43*, 1487−1497.
(37) Mayo, F. R.; Lewis, F. M. *J. Am. Chem. Soc.* **1944**, *66*, 1594−1601.
(38) Hoogenboom, R.; Fijten, M. W. M.; Wijnans, S.; van den Berg, A. M. J.; Thijs, H. M. L.; Schubert, U. S. *J. Comb. Chem.* **2006**, *8*, 145−148.
(39) Hoogenboom, R.; Schubert, U. S. *J. Polym. Sci., Part A: Polym. Chem.* **2003**, *41*, 2425−2434.
(40) Hoogenboom, R.; Fijten, M. W. M.; Thijs, H. M. L.; van Lankvelt, B. M.; Schubert, U. S. *Des. Monomers Polym.* **2005**, *8*, 659−671.
(41) Young, R. J.; Lovell, P. A. *Introduction to Polymers*, 2nd ed.; Chapman & Hall: London, 1991.
(42) Hayes, S. A.; Goruppa, A. A.; Jones, F. R. *J. Mater. Res.* **2004**, *19*, 3298−3306.
(43) Elias, H.-G. *An Introduction to Polymer Science*, 1st ed.; VCH: Weinheim, Germany, 1997.
(44) Tweedie, C. A.; Van Vliet, K. J. *J. Mater. Res.* **2006**, *21*, 1576−1589.
(45) Donth, E.; Beiner, M.; Reissig, S.; Korus, J.; Garwe, F.; Vieweg, S.; Kahle, S.; Hempel, E.; Schroter, K. *Macromolecules* **1996**, *29*, 6589−6600.
(46) Some quasi-static indentation moduli displayed in Figure 8B for the random copolymers should be treated with circumspection: for 33 and 67 wt % NonOx, the displacement during unloading is clearly not only governed by elastic material response: the ratio of the displacement rate at the start of the unloading to the displacement rate at the end of the hold period is only 1.8:1 and 4.6:1 for these two samples. Furthermore, for the random copolymers with 67, 75, and 82 wt % NonOx the result is based on only two, four, and five load−displacement responses, respectively, as the other responses (with higher maximum loads) were outside the depth range of the probe area function calibration.

MA070720R